Ammonia−Hydrogen Bromide and Ammonia−Hydrogen Iodide Complexes: Anion Photoelectron and ab Initio Studies†

S. N. Eustis,‡ A. Whiteside,§ D. Wang,‡ M. Gutowski,§,|| and K. H. Bowen*,‡

Department of Chemistry, Johns Hopkins University, Baltimore, Maryland 21218, Department of Chemistry, Heriot-Watt University, Edinburgh, EH14 4AS U.K., and Department of Chemistry, University of Gdańsk, 80-952 Gdańsk, Poland

Received: July 2, 2009; Revised Manuscript Received: August 5, 2009

The ammonia−hydrogen bromide and ammonia−hydrogen iodide, anionic heterodimers were studied by anion photoelectron spectroscopy. In complementary studies, these anions and their neutral counterparts were also investigated via ab initio theory at the coupled cluster level. In both systems, neutral $NH_3\cdots HX$ dimers were predicted to be linear, hydrogen-bonded complexes, whereas their anionic dimers were found to be proton-transferred species of the form, $(NH_4^+X^-)^-$. Both experimentally measured and theoretically predicted vertical detachment energies (VDE) are in excellent agreement for both systems, with values for $(NH_4^+Br^-)^-$ being 0.65 and 0.67 eV, respectively, and values for $(NH_4^+I^-)^-$ being 0.77 and 0.81 eV, respectively. These systems are discussed in terms of our previous study of $(NH_4^+Cl^-)^-$.

Introduction

Acid−base reactions between ammonia and hydrogen halides (HX) have fascinated generations of scientists, most of whom have seen the white fog that develops when vapors from ammonium hydroxide and hydrochloric acid intermingle. While reactions between ammonia and all the hydrogen halides readily form ammonium halide salts at significant reactant densities, their ability to proceed on the microscopic level with only one molecule of each reactant is another matter. Since the acidities of hydrogen halides increase consecutively from HF, to HCl, to HBr, to HI, the tendency for proton transfer to occur within the confines of isolated, neutral $NH_3\cdots HX$ complexes would also be expected to increase in that order. This expectation is somewhat quantified by the following semiempirical condition for proton transfer in neutral base$\cdots$HX complexes,[1] $PA_{base} + \Delta H_{acid} + 102 > 0$, where PA is the proton affinity of base, ΔH_{acid} is the acidity of HX (the negative of the enthalpy of dissociation for the $HX \rightarrow H^+ + X^-$ reaction), and where both values are in units of kcal/mol. Applying this criterion to the $NH_3\cdots HX$ series yields negative values in all four cases, viz., −65.4, −27.4, −17.4, and −8.3, where HX = HF, HCl, HBr, and HI, respectively. Furthermore, this outcome is consistent with the preponderance of available experimental data and high level calculations on neutral $NH_3\cdots HX$ complexes; i.e., proton transfer between NH_3 and HX in an isolated interacting pair does not occur. Below, we briefly summarize the pertinent literature on $NH_3\cdots HCl$, $NH_3\cdots HBr$, and $NH_3\cdots HI$ neutral complexes.

In the case of NH_3 and HCl, early theoretical work suggested that their reaction would proceed with only a single molecule of each reactant.[2] Later theoretical studies, however, found that hydrogen bonding rather than proton transfer would likely dominate in complexes of ammonia and hydrogen chloride.[3,4] Experimental work including pulsed nozzle, Fourier-transform microwave studies,[5,6] matrix-isolated infrared investigations,[7−10] and Stark effect measurements[11] have since provided conclusive evidence that the neutral NH_3/HCl pair does not undergo proton transfer, preferring instead to form the linear hydrogen-bonded complex, $NH_3\cdots HCl$. Modern theoretical predictions[12−21] are in accord with these results.

Fourier-transform microwave work showed the $NH_3\cdots HBr$ complex to be predominantly hydrogen-bonded but with 11% ionic character.[6,22] Stark effect measurements were consistent with a linear, hydrogen bonded complex.[11] Matrix-isolated infrared studies in which NH_3 and HBr were codeposited with the relatively nonperturbing host, neon, found the NH_3/HBr pair to form a hydrogen-bonded complex.[23−25] However, with more interactive hosts, such as Ar, Kr, and N_2, the infrared spectra were consistent with a growing degree of proton-transfer character in the $NH_3\cdots HBr$ complex.[25] Thus, the matrix environment was found to significantly influence the extent of proton transfer in the $NH_3\cdots HBr$ complex. Theoretical work was consistent with these experimental results, finding the isolated NH_3/HBr pair to form a linear, hydrogen-bonded complex with little to no proton transfer.[4,20,26−28]

While Fourier-transform microwave work suggested that the $NH_3\cdots HI$ complex is hydrogen-bonded rather than proton transferred,[6,29,30] matrix-isolated infrared studies found the level of proton transfer to be entirely dependent on the host.[31−33] Furthermore, different calculations found various degrees of proton transfer within the $NH_3\cdots HI$ complex,[26,27,34] these ranging from none to complete proton transfer. Clearly, the $NH_3\cdots HI$ complex is edging toward proton transfer even in the gas phase, and it is quite sensitive to changes in its environment.

Thus, in isolation, proton transfer does not spontaneously occur between a single molecule of ammonia and a single molecule of any of the three hydrogen halides considered here; these reactions, which occur so readily in bulk, do not have a true molecular level (two body) counterpart. Instead, they require the aid of external interactions, albeit to different extents, to initiate proton transfer and form ionic ammonium halides, $NH_4^+X^-$.

† Part of the "W. Carl Lineberger Festschrift".

* Corresponding author. E-mail: kbowen@jhu.edu.
‡ Johns Hopkins University.
§ Heriot-Watt University. E-mail: M.G., m.gutowski@hw.ac.uk.
|| University of Gdańsk.

10.1021/jp906238v
Published on Web 09/04/2009

Among the simplest of perturbing agents is an electron, and through a combination of anion photoelectron spectroscopic experiments and high level ab initio calculations, in a previous study we showed that an excess electron is indeed enough to initiate proton transfer between ammonia and hydrogen chloride, forming the anion of ammonium chloride.[21] Our work further showed that the excess electron occupies a highly delocalized orbital surrounding the NH_4^+ cation, creating a Rydberg NH_4 moiety that itself interacts with and is distorted by the neighboring chloride anion, i.e., $(NH_4^+Cl^-)^- = NH_4\cdots Cl^-$. Thus, while the most stable form of the isolated neutral complex is likely hydrogen-bonded, the anionic complex prefers a proton-transferred configuration.

Our work with this system led us to examine analogous complexes between ammonia and the heavier hydrogen halides, HBr and HI. Two effects must be considered in the progression through the halogens. First, the larger halogens are better proton donors, which will affect the energetics of the electron-driven proton transfer. Second, the larger halogens show a tendency to form halogen bonds, resulting in a stable $NH_3\cdots XH$ complex. However, due to dipole cancellation, such a complex would only weakly bind electrons, and would not undergo electron-driven proton transfer. Therefore this result will be discussed in a later publication.

Here, we present a synergetic experimental (anion photoelectron spectroscopy) and theoretical (coupled cluster level) study of both the anions and the corresponding neutral forms of ammonia−hydrogen bromide and ammonia−hydrogen iodide complexes.

Experimental Section

Anion photoelectron spectroscopy is conducted by crossing a mass-selected beam of negative ions with a fixed-frequency photon beam and energy-analyzing the resultant photodetached electrons. Photodetachment is governed by the energy-conserving relationship, $h\nu = \mathrm{EBE} + \mathrm{EKE}$, where $h\nu$ is the photon energy, EBE is electron binding energy, and EKE is electron kinetic energy. Knowing the photon energy and measuring the electron kinetic energy lead to the electron binding energies of the observed transitions.

The anionic complexes of interest were generated in a nozzle-ion source. In this device an ammonia/argon mixture (15%/85%) at 1−3 atm and 25 °C was expanded through a 20 μm orifice (nozzle) into an operating vacuum of $\sim 7 \times 10^{-5}$ Torr, while an HX/argon (10%/90%) mixture at a few Torr was allowed to infuse into the expansion region immediately outside the nozzle. The stagnation chamber and nozzle were biased at −500 V. Low energy electrons from an independently biased, thoriated-iridium filament were directed into the jet near the mouth of the nozzle. An axial magnetic field helped to form a microplasma just outside the nozzle orifice. Anions formed in this way were extracted through a 2 mm diameter skimmer into the ion optical system of the spectrometer. These were mass-analyzed by a 90° sector magnet (mass resolution = 400) before being mass-selected and directed into the ion-photon interaction region, where they interacted with ~200 circulating W of 2.540 eV photons from an argon ion laser operated intracavity. The resulting photodetached electrons were analyzed by a hemispherical electron energy analyzer (constant resolution throughout energy window) and counted by an electron multiplier. The photoelectron spectra were calibrated against the well-known photoelectron spectrum of O^-. Our apparatus has been described in detail previously.[35]

Theoretical Section

The coupled cluster electronic structure method was used due to the significant contribution of electron correlation effects to the stability of weakly bound excess electron systems.[36,37] Geometry optimizations, dipole moment calculations, and vibrational zero-point energy corrections were performed at the coupled-cluster singles-doubles level of theory (CCSD) with tight energy convergence criteria. Single-point energy calculations were performed with perturbative triples (CCSD(T)), using the same basis sets, geometries, and tight convergence criteria.

The large, diffuse SOMO orbital in the anion would not be correctly described by conventional basis sets, even those augmented with conventional diffuse functions. Therefore the augmented, polarized, correlation-consistent basis set of double-ζ quality[38−40] was supplemented with an additional set of seven s and seven p diffuse functions.[41] The additional diffuse s and p functions were "even-tempered"; i.e., their exponents form geometric progressions with the progression constant set to 2.5, and they used the most diffuse s and p functions on the conventional basis set as the zeroth functions in each progression. These extra functions are centered on the positive end of the complex's dipole, in this instance, on the nitrogen atom. Hereafter, these basis sets are referred to as "aug-cc-pvdz-2.5". Iodine, however, is an exception; there, the aug-cc-pvdz-PP basis set[42] (relativistic pseudopotentials for the core electrons on iodine) was used. All calculations were performed in the Gaussian 03 package.[43] Visualizations of molecules were generated in MOLDEN[44] with diffuse orbitals visualized as 50%-of-electron iso-surfaces using VMD[45] and OpenCubMan.[46]

Adiabatic electron affinities (EA_a) for neutrals were computed as the energy of the anions subtracted from the energy of the neutrals at their optimized geometries, with zero-point energy corrections applied. Positive values therefore indicate that binding of an electron is exothermic, i.e., the standard thermochemical definition. Vertical (electron) detachment energies (VDE) for anions were determined as the energy of the anion at its optimized geometry subtracted from the energy of the neutral at the same geometry. Likewise, vertical electron (attachment) affinities (EA_V) were computed as the energy of the anion at the neutral's optimized geometry, subtracted from the energy of the neutral at that same geometry. Positive values indicate that the anionic state is bound with respect to the neutral.

Dissociation energies were determined as the energy of the relevant complex at its optimized geometry subtracted from the sum of the energies of its two separated fragments at their optimized geometries. The energy of the complex was determined using the dimer-centered basis set, with BSSE (by counterpoise) and vibrational zero-point energy corrections applied. Likewise, the monomer energies were determined with monomer-centered basis sets with vibrational zero-point corrections. Positive values indicate that fragmenting the complex is an endothermic process.

Proton affinities were determined as the energies of the protonated species subtracted from those of the deprotonated species at their optimized geometries, with (where necessary) zero-point energy and counterpoise corrections included. Positive values indicate that binding a proton is exothermic.

Relaxed potential energy curves for neutrals were calculated at the CCSD level with the aug-cc-pvdz-2.5 basis set described previously. The acidic proton, aligned with the C_3 axis and bridging the heavy atoms, is dubbed as "shuttling" because its position is profoundly affected by the excess electron attachment. The "shuttling" proton position was varied and all other coordinates relaxed. This proton's position is explicitly relative

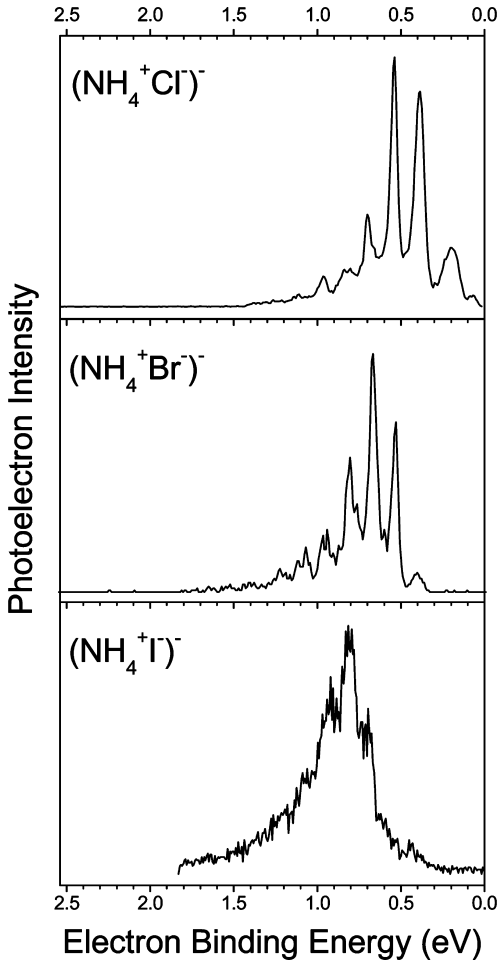

Figure 1. Photoelectron spectra of the ammonium chloride anion, the ammonium bromide anion, and the ammonium iodide anion each taken with 2.540 eV photons. The spectrum of the ammonium chloride anion[21] is presented here for comparison.

to either the nitrogen or the halogen, which each give a unique potential energy surface. At intermediate distances, the choice of coordinate does not influence the result, and the surfaces are identical. As the shuttling coordinate is extended, the other heavy atom is free to retreat from the advancing proton. Therefore we do not probe the proton shuttling potential energy surface near the other heavy atom but instead probe the heavy atom−heavy atom breathing potential energy surface. For example at a high halogen−proton distance, the proton−nitrogen distance becomes constant, and the nitrogen−halogen distance varies. This was circumvented by combining surfaces created using both coordinates.

The potential energy curve for the anion was assessed as the vertical attachment energy at each point of the neutral potential energy curve, in order that the vertically bound or unbound nature of the anion would be obvious. This also avoided anticipated difficulties with spontaneous autodetachment of the electron during optimization in the weakly bound region of the surface.

Results

The measured photoelectron spectra of $(NH_4^+Cl^-)^-$, $(NH_4^+Br^-)^-$, and $(NH_4^+I^-)^-$ are presented in Figure 1. Peak centers (EBE) for each of these spectra are tabulated in Table 1. Experimental and calculated values for vertical detachment energies (VDE) and electron affinities (EA_a) are presented in Table 2. Computed structures for the anions and their neutral counterparts are presented in Figure 2. In Table 3, the nitrogen−hydrogen and the halogen−hydrogen bond lengths in the free ammonium cation and the free hydrogen halides, respectively, are compared to the nitrogen-"shuttling proton" and the halogen-"shuttling proton" bond lengths in both the neutral and anionic structures of the complexes under study here. Theoretical potential energy curves are presented in Figures 3 and 4.

TABLE 1: Experimental Peak Center Positions (EBE's) for the Photoelectron Spectra, $(NH_4^+X^-)^-$ (X = Cl, Br, I)[a]

v'	$(NH_4^+Cl^-)^-$	$(NH_4^+Br^-)^-$	$(NH_4^+I^-)^-$
1	0.075		0.451
2	0.196	0.402	0.619
3	0.384	0.530	0.696
4	0.537	0.667	0.814
5	0.700	0.804	0.920
6	0.802	0.941	1.060
7	0.965	1.069	1.179
8		1.223	

[a] All Data are in eV. $(NH_4^+Cl^-)^-$ data are taken from ref 21.

The photoelectron spectra of $(NH_4^+Br^-)^-$ and $(NH_4^+I^-)^-$, though different from one another, are nevertheless reminiscent of the spectrum of $(NH_4^+Cl^-)^-$, which we collected in our previous study.[21] The spectrum of $(NH_4^+Br^-)^-$ reveals a clear vibrational progression beginning with a peak at EBE ~0.4 eV and with the maximum in its fitted intensity envelope occurring at 0.67 eV. The spectrum of $(NH_4^+I^-)^-$ is similar in shape, with a maximum intensity occurring at 0.81 eV. In neither case did the spectral patterns change with source conditions, suggesting that none of the observed peaks are due to vibrational hot bands. While all of these ammonium halide anion photoelectron spectra are analogous to alkali halide anion photoelectron spectra in that they are anions of salts,[47] they are different in that the formation of ammonium halide anions involves proton transfers and in that the vibrational structure in their spectra are primarily due to shuttling proton motions. The related vibrational mode is a fully symmetric stretching mode dominated by the motion of the "shuttling proton" along the C_3 axis, mirroring our earlier assessment of this motion in the case of the $(NH_4^+Cl^-)^-$ system.[21]

The results of our theoretical studies on these two systems are consistent with our experimental results. Theory predicts that for both systems the neutral complexes are linear and hydrogen-bonded, whereas for both anionic complexes the preferred configuration is the proton transferred ionic salt, $(NH_4^+X^-)^-$. As shown in Table 3, the halogen−hydrogen distances in the neutral complexes, although extended, are close to those of the free hydrogen halide. However, the distance from the nitrogen to the shuttling proton in each neutral complex is substantially larger than a nitrogen−hydrogen bond in the free ammonium cation. This indicates a covalently bonded hydrogen halide that is noncovalently bonded to an ammonia molecule. Conversely, in the anions, the distance from the nitrogen to the shuttling proton is close to that seen in the ammonium cation, albeit slightly elongated. Furthermore, the distance from the halogen atom to this proton is much larger than that in the free hydrogen halides. This implies that the proton has been fully transferred and covalently bonded by the nitrogen, and that a noncovalent interaction exists between that hydrogen and the halide anion.

In the case of $(NH_4^+Br^-)^-$, there is excellent agreement between the experimental and theoretical VDE values (0.67 ±

TABLE 2: Experimental and Theoretical Electron Affinities (EA_a) and Vertical Detachment Energies (VDE) for the $NH_3\cdots HBr/(NH_4^+Br^-)^-$ and the $NH_3\cdots HI/(NH_4^+I^-)^-$ Systems[a]

	$NH_3\cdots HBr$	$(NH_4^+Br^-)^-$	$NH_3\cdots HI$	$(NH_4^+I^-)^-$	$NH_3\cdots HCl$	$(NH_4^+Cl^-)^-$
expt VDE		0.67		0.81		0.540
theo VDE		0.65		0.77		0.52
expt EA_a	0.28		0.45		0.075	
theo EA_a	0.26		0.47		0.068	

[a] All Data are in eV. $NH_3\cdots HCl/(NH_4^+Cl^-)^-$ data are taken from ref 21.

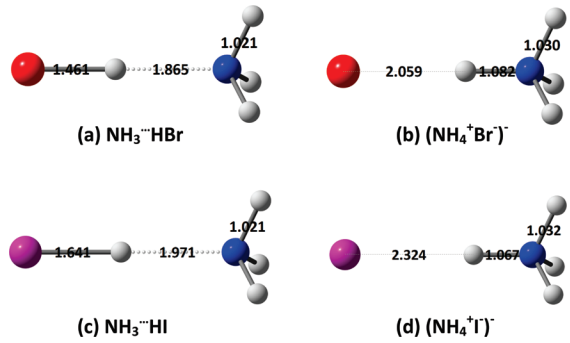

Figure 2. Calculated geometries for (I) $NH_3\cdots HBr$, (II) $(NH_4^+Br^-)^-$, (III) $NH_3\cdots HI$, and (IV) $(NH_4^+I^-)^-$ at the CCSD/aug-cc-pvdz-2.5 level of theory. Key: blue for nitrogen, white for hydrogen, red for bromine, purple for iodine.

TABLE 3: Computed Nitrogen−Hydrogen and Halogen−Hydrogen Distances (Å) for Neutral and Anionic Complexes Compared to Computed Values for the Free Ammonium Cation and the Free Hydrogen Halides[a]

	$NH_3\cdots HBr$	$(NH_4^+Br^-)^-$	$NH_3\cdots HI$	$(NH_4^+I^-)^-$
$\Delta(N-H_s)$	+0.836	+0.053	+0.943	+0.039
$\Delta(X-H_s)$	+0.036	+0.634	+0.028	+0.714

[a] The hydrogen atoms being referred to here are the "shuttling protons", H_s, in both $\Delta(N-H_s)$ and $\Delta(X-H_s)$. Positive values indicate greater distances in the complex.

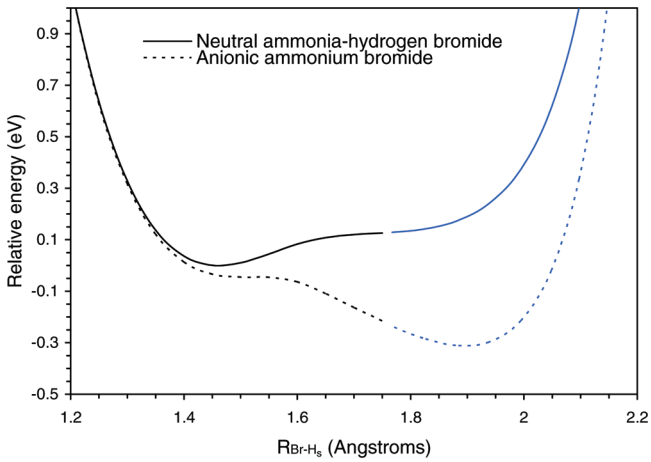

Figure 3. Potential energy surfaces for the $(NH_4^+Br^-)^-$ anionic and the $NH_3\cdots HBr$ neutral complexes at the CCSD/aug-cc-pvdz-2.5 level of theory, dashed and solid lines, respectively. Black indicates the surface evaluated from the proton−halogen distance; blue indicates the surface evaluated from the proton-nitrogen distance.

0.02 eV vs 0.65 eV, respectively). Initial assignments for the adiabatic electron affinity (EA_a) of ammonium bromide focused on the first visible peak centered at EBE = 0.41 eV. However, by subtracting the nearest vibrational spacing (0.131 eV) from the peak center at EBE = 0.41 eV, we arrived at a value of 0.28 eV, which is consistent with the theoretically proposed value of 0.26 eV for the EA_a value of ammonium bromide.

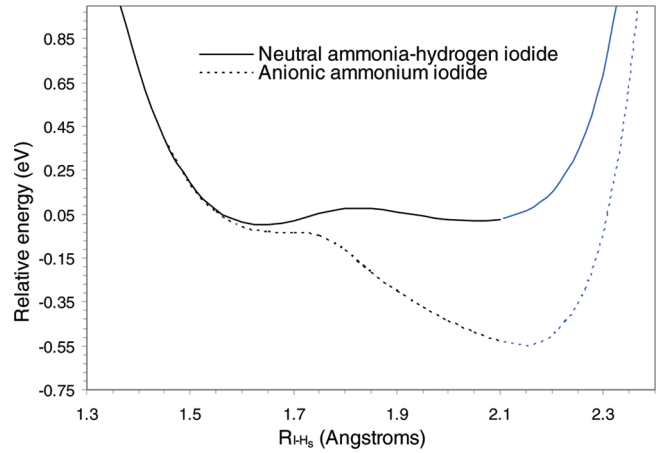

Figure 4. Potential energy surfaces for the $(NH_4^+I^-)^-$ anionic and the $NH_3\cdots HI$ neutral complexes calculated at the CCSD/aug-cc-pvdz-2.5 level, dashed and solid lines, respectively. Colors as in Figure 3.

Furthermore, upon careful comparison of the peak patterns in the $(NH_4^+Cl^-)^-$ and the $(NH_4^+Br^-)^-$ photoelectron spectra, one sees that the $(NH_4^+Br^-)^-$ spectrum is missing the lowest EBE (origin) peak seen in the $(NH_4^+Cl^-)^-$ spectrum. This is likely caused by the relatively lower signal-to-noise ratio of the $(NH_4^+Br^-)^-$ spectrum as compared to the $(NH_4^+Cl^-)^-$ spectrum. On the basis of the foregoing, we put forth 0.28 ± 0.05 eV as the best value for the EA_a of ammonium bromide.

In the case of $(NH_4^+I^-)^-$, we again find excellent agreement between the experimental and calculated values of the VDE (0.81 ± 0.04 and 0.77 eV, respectively). In this case, the theoretically proposed EA_a value of 0.47 eV is consistent with the weak peak centered at EBE ∼ 0.45 eV. We thus take the EA_a to be 0.45 ± 0.05 eV. Interestingly, despite a relatively strong $(NH_4^+I^-)^-$ ion signal, its photoelectron spectrum was weak by comparison with those of $(NH_4^+Cl^-)^-$ and $(NH_4^+Br^-)^-$, revealing a photodetachment cross section for $(NH_4^+I^-)^-$ that is roughly 10 times less than that of $(NH_4^+Cl^-)^-$. (The fact that the photoelectron spectrum of $(NH_4^+Br^-)^-$ has a slightly lower signal-to-noise ratio than that of $(NH_4^+Cl^-)^-$ is mostly due to a lower $(NH_4^+Br^-)^-$ ion intensity rather than to a lower photodetachment cross section.)

Discussion

The results provide strong evidence that the anionic complexes of ammonia−hydrogen bromide and ammonia−hydrogen iodide are, in fact, the anions of the salts, $(NH_4^+Br^-)^-$ and $(NH_4^+I^-)^-$. Moreover, as in the ammonia−hydrogen chloride system reported previously,[21] their corresponding neutral complexes are linear and hydrogen-bonded, with little or no proton transfer. Consistent with these findings is the similarity, as mentioned above, between the photoelectron spectrum of $(NH_4^+Cl^-)^-$ and those of $(NH_4^+Br^-)^-$ and $(NH_4^+I^-)^-$. Comparing the experimental VDE and EA_a values, we see an increase from the chloride to the bromide case of 0.13 and 0.20 eV and

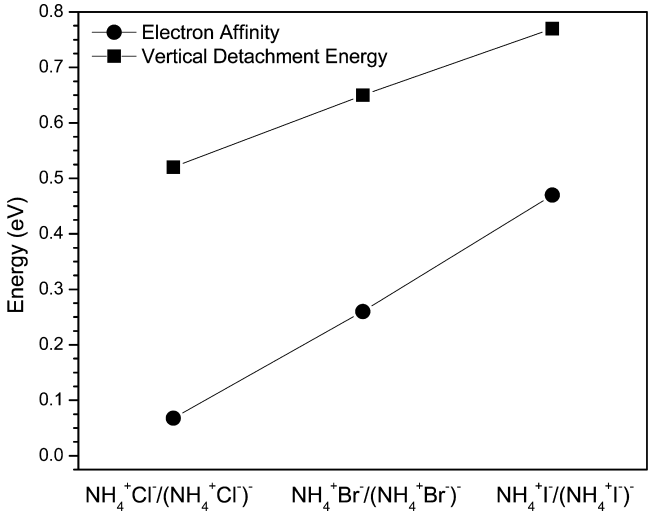

Figure 5. Comparison of computed EA_a and VDE values for $NH_3\cdots HCl$ and $(NH_4^+Cl^-)^-$, $NH_3\cdots HBr^-$ and $(NH_4^+Br^-)^-$, and $NH_3\cdots HI$ and $(NH_4^+I^-)^-$, respectively. Values for $NH_3\cdots HCl$ and $(NH_4^+Cl^-)^-$ were taken from ref 21.

from the bromide to the iodide case of 0.14 and 0.17 eV, respectively—a consistent yet relatively modest change. Similar comparisons are seen among the theoretically predicted VDE and EA_a values, and these are plotted in Figure 5. Both the $(NH_4^+Br^-)^-$ and the $(NH_4^+I^-)^-$ photoelectron spectra also show vibrational progressions due to the proton shuttling mode ($N\cdots H_s\cdots X$). The vibrational spacings for the most intense peaks have shrunk from 0.154 eV (1242 cm^{-1}) in the $(NH_4^+Cl^-)^-$ spectrum to 0.135 eV (1089 cm^{-1}) in the $(NH_4^+Br^-)^-$ spectrum, largely reflecting the greater mass of bromine over chlorine. The vibrational spacings in the $(NH_4^+I^-)^-$ spectrum follow the same trend. The local minimum in the neutral potential energy surface of NH_3HI (Figure 4) around the proton-transferred geometry should be noted. This has a depth of approximately 50 meV. As the structure of the spectrum arises from the formation of a vibrationally excited neutral in this region of the potential energy surface upon removal of the electron, this complication may contribute to the poor resolution of the vibrational structure.

Conceptually, the fact that proton transfer is made favorable by the addition of an excess electron can be rationalized in terms of the stabilization of the excess electron by the increased dipole moment on the ionic system versus the hydrogen-bonded one. This can be visualized by comparing the two plots in Figure 6, these depicting the volumes of 50% electron isosurfaces for the LUMO of neutral $NH_3\cdots HBr$ and for the SOMO of anionic $(NH_4^+Br^-)^-$.

Insight is also provided by considering the energetics of these systems. For example, consider forming the separated NH_4^+/Cl^- ion pair from NH_3 and HCl molecules. For proton transfer between the gas-phase, noninteracting acid and base, i.e., the transformation from $NH_3 + HCl$ to $NH_4^+ + Cl^-$ shown in Figure 7, the energy needed is the difference in the gas-phase proton affinities of ammonia and the chloride anion, calculated as 5.37 eV (5.58 eV, if we correct for zero-point energy and counterpoise). However, the transformation from the $H_3N\cdots HCl$ neutral complex to the net neutral $H_3NH^{+\cdots}Cl^-$ salt requires only 0.38 eV. This is a much lower energy than the proton transfer between the two isolated fragments. (Here, we used our a priori knowledge of the proton-transferred structure and disregarded the unavailable zero-point vibrational energy.)

The reason for this is that the energy recovered by associating the ammonium chloride ion pair ($NH_4^+ + Cl^-$ to $H_3NH^+\cdots Cl^-$)

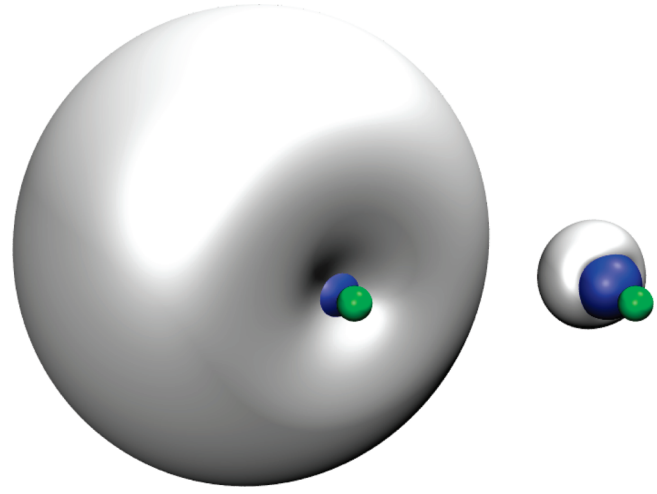

Figure 6. Plots depicting the volumes of 50% electron isosurfaces for the LUMO of neutral $NH_3\cdots HBr$ on the left and for the SOMO of anionic $(NH_4^+Br^-)^-$ on the right.

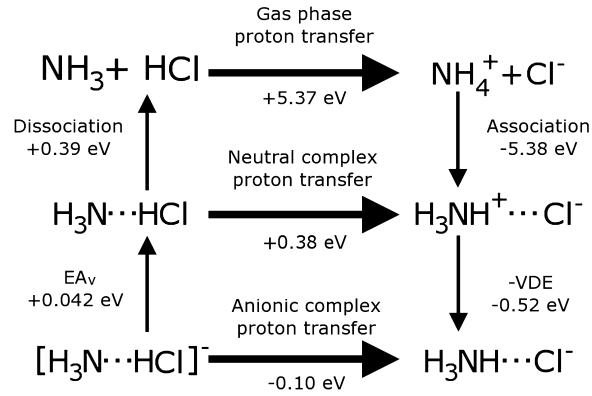

Figure 7. Energetic cycles relating to the formation of the ammonium chloride anion.

is significantly more than the energy needed to dissociate the ammonia−hydrogen chloride, hydrogen bonded, neutral complex ($H_3N\cdots HCl$ to $NH_3 + HCl$). The difference in dissociation energies is 4.99 eV (4.97 eV with counterpoise, ZPE unavailable for $NH_4^+Cl^-$). If we traverse the diagram, we can see that the extra electrostatic stability accounts for the bulk of the energy needed to transfer the proton, dropping the endothermicity by 4.99 eV from 5.37 to 0.38 eV. However, proton transfer is still not spontaneous in the neutral.

The situation changes qualitatively with the addition of an excess electron. It can be seen that the vertical attachment energy of the excess electron to the neutral complex (EA_v = 0.042 eV, $H_3N\cdots HCl$ to $[H_3N\cdots HCl]^-$) is significantly lower than the vertical detachment energy from the anionic complex (VDE = 0.52 eV, $H_3NH^{\cdots}Cl^-$ to $H_3NH^+\cdots Cl^-$). That is to say, the extra electron is more stable by 0.482 eV when the anionic complex is of the ionic, proton-transferred type. This makes intuitive sense, given the larger dipole moment in the ionic form (4.31 D for the neutral at the hydrogen-bonded geometry, versus 10.01 D for the neutral at the ionic geometry). It is this extra 0.482 eV stabilization that "tips the balance" in favor of the electron-induced, proton transfer process, from endothermic by 0.38 eV to exothermic by 0.10 eV.

This scenario also holds for the bromide and the iodide. Similar schemes are provided in Figures 8 and 9. Comparing the ammonia−hydrogen bromide complex to the ammonia−hydrogen chloride complex, a lessened proton affinity difference

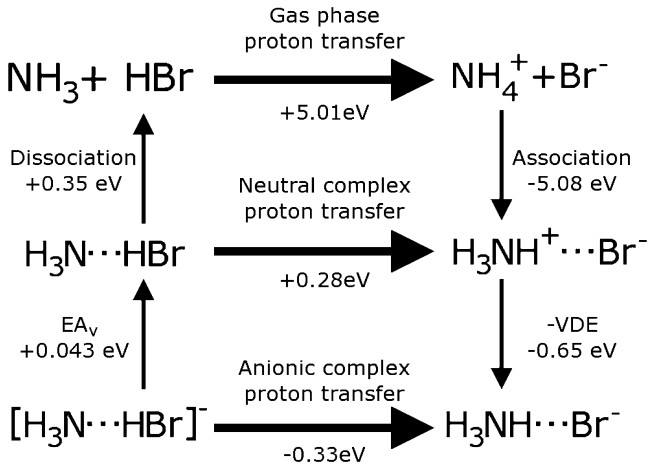

Figure 8. Energetic cycles relating to the formation of the ammonium bromide anion.

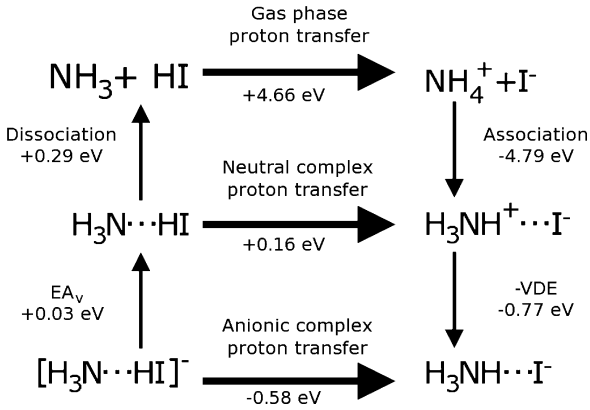

Figure 9. Energetic cycles relating to the formation of the ammonium iodide anion.

of 5.01 eV (5.20 eV with counterpoise and ZPE corrections) is partially counterbalanced by a lowered dissociation energy difference of 4.73 eV (4.69 eV with counterpoise), leaving a reduced endothermicity of 0.28 eV to proton transfer in the neutral complex. Formation of the ionic complex in the anion stabilizes the excess electron by 0.65 eV, resulting in an exothermicity of −0.33 eV for proton transfer in the anionic complex. The neutral dipole moment at the hydrogen-bonded geometry is 4.20 D, while that at the ionic geometry is 10.95 D.

For iodine, the proton affinity difference is 4.66 eV (4.83 eV), with the dissociation energy difference for the neutral, ionic complex 4.50 eV (4.43 eV) higher than that of the hydrogen-bonded, neutral complex, resulting in a 0.16 eV endothermicity for proton transfer in the neutral complex. Forming the ionic complex in the anion stabilizes the excess electron by a net 0.74 eV, i.e., −0.77 to +0.03 eV, resulting in an exothermicity of −0.58 eV for proton transfer in the anionic complex. The neutral dipole moments are 3.74 and 11.69 D for the hydrogen-bonded and ionic geometries, respectively.

Note that proton transfer in the neutral complexes approaches spontaneity in all three systems as the halogen size, and thus acidity, increases. With increasing halogen size, the hydrogen halide becomes a stronger acid, and therefore proton transfer in the neutral becomes less endothermic. Therefore, it is expected that proton transfer will become spontaneous in the neutral with slightly stronger bases or acids than those considered here.

Furthermore, as reflected in both the experimental and the theoretical results, the stabilization of the excess electron, brought on by forming the anionic ionic complex, grows with increasing halogen size, making electron-induced proton transfer increasingly exothermic. This is the dominant contribution to the trend, This stabilization arises in part due to the declining dipole moments of the hydrogen-bonded, neutral complexes (4.31 D, 4.20 D, and 3.74 D for $NH_3\cdots HCl$, $NH_3\cdots HBr$, $NH_3\cdots HI$, respectively), and in part due to the increasing dipole moments of the ionic systems (10.01, 10.95, and 11.69 D for $NH_4^+Cl^-$, $NH_4^+Br^-$, and $NH_4^+I^-$, respectively). These, in turn, are due to the reduced polarization of the H−X bond in the hydrogen halides of the hydrogen-bonded complexes and to the increasing N−X distances in the ionic systems, respectively.

It is noteworthy from an "orbital taxonomy" perspective that in these proton transfer processes, the excess electron shifts from a distinctly dipole-bond orbital at the neutral equilibrium geometry to a much more compact orbital akin to a distorted valence s-orbital (forming the distorted NH_4 Rydberg molecular moiety) at the anion equilibrium geometry.

Acknowledgment. This material is based in part on work supported by National Science Foundation grant number, 0809258 (K.H.B.). We also thank the Polish State Committee for Scientific Research (KBN) for support under grant DS/8000-4-0026-9 (M.G). We further thank the EPSRC for a studentship (A.W.).

References and Notes

(1) Alkorta, I.; Rozas, I.; Mo, O.; Yanez, M.; Elguero, J. *J. Phys. Chem. A* **2001**, *105*, 7481.
(2) Clementi, E.; Gayles, J. N. *J. Chem. Phys.* **1967**, *47*, 3837.
(3) Latajka, Z.; Sakai, S.; Morokuma, K.; Ratajczak, H. *Chem. Phys. Lett.* **1984**, *110*, 464.
(4) Brciz, A.; Karpfen, A.; Lischka, H.; Schuster, P. *Chem. Phys.* **1984**, *89*, 337.
(5) Goodwin, E. J.; Howard, N. W.; Legon, A. C. *Chem. Phys. Lett.* **1986**, *131*, 319.
(6) Legon, A. C. *Chem. Soc. Rev.* **1993**, *22*, 153.
(7) Ault, B. S.; Pimentel, G. C. *J. Phys. Chem.* **1973**, *77*, 1649.
(8) Andrews, L.; Wang, X. F.; Mielke, Z. *J. Am. Chem. Soc.* **2001**, *123*, 1499.
(9) Andrews, L.; Wang, X. F.; Mielke, Z. *J. Phys. Chem. A* **2001**, *105*, 6054.
(10) Barnes, A. J.; Legon, A. C. *J. Mol. Struct.* **1998**, *448*, 101.
(11) Brauer, C. S.; Craddock, M. B.; Kilian, J.; Grumstrup, E. M.; Orilall, M. C.; Mo, Y. R.; Gao, J. L.; Leopold, K. R. *J. Phys. Chem. A* **2006**, *110*, 10025.
(12) Corongiu, G.; Estrin, D.; Murgia, G.; Paglieri, L.; Pisani, L.; Valli, G. S.; Watts, J. D.; Clementi, E. *Int. J. Quantum Chem.* **1996**, *59*, 119.
(13) Ramos, M.; Alkorta, I.; Elguero, J.; Golubev, N. S.; Denisov, G. S.; Benedict, H.; Limbach, H. H. *J. Phys. Chem. A* **1997**, *101*, 9791.
(14) Cazar, R.; Jamka, A.; Tao, F. M. *Chem. Phys. Lett.* **1998**, *287*, 549.
(15) Cazar, R. A.; Jamka, A. J.; Tao, F. M. *J. Phys. Chem. A* **1998**, *102*, 5117.
(16) Del Bene, J. E.; Jordan, M. J. T. *J. Chem. Phys.* **1998**, *108*, 3205.
(17) Tao, F. M. *J. Chem. Phys.* **1999**, *110*, 11121.
(18) Jordan, M. J. T.; Del Bene, J. E. *J. Am. Chem. Soc.* **2000**, *122*, 2101.
(19) Cherng, B.; Tao, F. M. *J. Chem. Phys.* **2001**, *114*, 1720.
(20) Biczysko, M.; Latajka, Z. *J. Phys. Chem. A* **2002**, *106*, 3197.
(21) Eustis, S. N.; Radisic, D.; Bowen, K. H.; Bachorz, R. A.; Haranczyk, M.; Schenter, G. K.; Gutowski, M. *Science* **2008**, *319*, 936.
(22) Howard, N. W.; Legon, A. C. *J. Chem. Phys.* **1987**, *86*, 6722.
(23) Ault, B. S.; Steinback, E.; Pimentel, G. C. *J. Phys. Chem.* **1975**, *79*, 615.
(24) Barnes, A. J.; Wright, M. P. *J. Chem. Soc., Faraday Trans.* **1986**, *82*, 153.
(25) Andrews, L.; Wang, X. F. *J. Phys. Chem. A* **2001**, *105*, 6420.
(26) Jasien, P. G.; Stevens, W. J. *Chem. Phys. Lett.* **1986**, *130*, 127.
(27) Latajka, Z.; Scheiner, S.; Ratajczak, H. *Chem. Phys.* **1992**, *166*, 85.
(28) Ruizlopez, M. F.; Bohr, F.; Martinscosta, M. T. C.; Rinaldi, D. *Chem. Phys. Lett.* **1994**, *221*, 109.
(29) Legon, A. C.; Stephenson, D. *J. Chem. Soc., Faraday Trans.* **1992**, *88*, 761.

(30) Legon, A. C. *J. Mol. Struct.* **1992**, *266*, 21.
(31) Schriver, L.; Schriver, A.; Perchard, J. P. *J. Am. Chem. Soc.* **1983**, *105*, 3843.
(32) Schriver, L. *Spectrochim. Acta A* **1987**, *43*, 1155.
(33) Andrews, L.; Wang, X. F. *J. Phys. Chem. A* **2001**, *105*, 7541.
(34) Kollman, P.; Dearing, A.; Kochanski, E. *J. Phys. Chem.* **1982**, *86*, 1607.
(35) Coe, J. V.; Snodgrass, J. T.; Freidhoff, C. B.; Mchugh, K. M.; Bowen, K. H. *J. Chem. Phys.* **1987**, *87*, 4302.
(36) Gutowski, M.; Skurski, P.; Boldyrev, A. I.; Simons, J.; Jordan, K. D. *Phys. Rev. A* **1996**, *54*, 1906.
(37) Gutowski, M.; Jordan, K. D.; Skurski, P. *J. Phys. Chem. A* **1998**, *102*, 2624.
(38) Dunning, T. H. *J. Chem. Phys.* **1989**, *90*, 1007.
(39) Kendall, R. A.; Dunning, T. H.; Harrison, R. J. *J. Chem. Phys.* **1992**, *96*, 6796.
(40) Woon, D. E.; Dunning, T. H. *J. Chem. Phys.* **1993**, *98*, 1358.
(41) Skurski, P.; Gutowski, M.; Simons, *J. Int. J. Quant. Chem.* **2000**, *80*, 1024.
(42) Peterson, K. A.; Figgen, D.; Goll, E.; Stoll, H.; Dolg, M. *J. Chem. Phys.* **2003**, *119*, 11113.
(43) Frisch, M. J.; Trucks, G. W.; Schlegel, H. B.; Scuseria, G. E.; Robb, M. A.; Cheeseman, J. R.; Montgomery, J. A., Jr.; Vreven, T.; Kudin, K. N.; Burant, J. C.; Millam, J. M.; Iyengar, S. S.; Tomasi, J.; Barone, V.; Mennucci, B.; Cossi, M.; Scalmani, G.; Rega, N.; Petersson, G. A.; Nakatsuji, H.; Hada, M.; Ehara, M.; Toyota, K.; Fukuda, R. Hasegawa, J.; Ishida, M. Nakajima, T.; Honda, Y. Kitao, O.; Nakai, H.; Klene, M.; Li, X.; Knox, J. E.; Hratchian, H. P.; Cross, J. B.; Bakken, V.; Adamo, C.; Jaramillo, J.; Gomperts, R.; Stratmann, R. E.; Yazyev, O.; Austin, A. J.; Cammi, R.; Pomelli, C.; Ochterski, J. W.; Ayala, P. Y.; Morokuma, K. Voth, G. A.; Salvador, P.; Dannenberg, J. J.; Zakrzewski, V. G.; Dapprich, S.; Daniels, A. D.; Strain, M. C.; Farkas, O.; Malick, D. K.; Rabuck, A. D. Raghavachari, K.; Foresman, J. B.; Ortiz, J. V.; Cui, Q.; Baboul, A. G.; Clifford, S.; Cioslowski, J.; Stefanov, B. B.; Liu, G. Liashenko, A.; Piskorz, P.; Komaromi, I.; Martin, R. L.; Fox, D. J.; Keith, T.; Al-Laham, M. A. Peng, C. Y.; Nanayakkara, A.; Challacombe, M.; Gill, P. M. W.; Johnson, B.; Chen, W.; Wong, M. W.; Gonzalez, C.; Pople, J. A. *Gaussian 03.C02*; Gaussian, Inc.: Wallingford, CT, 2004.
(44) Schaftenaar, G.; Noordik, J. H. *J. Comp. Aided Mol. Des.* **2000**, *14*, 123.
(45) Humphrey, W.; Dalke, A.; Schulten, K. *J. Mol. Graph.* **1996**, *14*, 33.
(46) Haranczyk, M.; Gutowski, M. *J. Chem. Theo. Comput.* **2008**, *4*, 689.
(47) Miller, T. M.; Leopold, D. G.; Murray, K. K.; Lineberger, W. C. *J. Chem. Phys.* **1986**, *85*, 2368.

JP906238V